REFERENCES

[1] R. B. Hammond, G. L. Hey-shipton, and G. L. Matthaei, "Designing with superconductors," *IEEE Spectrum*, pp. 34–39, Apr. 1993.

[2] D. Nghiem, J. T. Williams, and D. R. Jackson, "A general analysis of propagation along multi-layer superconducting stripline and strip transmission lines," *IEEE Trans. Microwave Theory Tech.*, vol. 39, no. 9, pp. 1553–1565, Sept. 1991.

[3] W. Lin, "A critical study of the coaxial transmission line utilizing conductors of both circular and square cross sections," *IEEE Trans. Microwave Theory Tech.*, vol. 30, no. 11, pp. 1981–1988, 1982.

[4] T. Itoh, "Spectral domain immitance approach for dispersion characteristics of generalized printed transmission lines," *IEEE Trans. Microwave Theory Tech.*, vol. MTT-28, no. 7, pp. 733–736, July 1980.

[5] J. C. Swihart, "Field solution for a thin-film superconducting strip transmission line," *J. Appl. Phys.*, vol. 32, no. 3, Mar. 1961, pp. 461–469.

[6] C. Wilker *et al.*, "5 GHz High-temperature-superconductor resonators with high Q and low power dependence up to 90 K," *IEEE Trans. Microwave Theory Tech.*, vol. 39, no. 9, pp. 1462–1467, Sept. 1991.

Characterization of Off-Slot Discontinuity in Unilateral Fin Line

Alok Kumar Gupta and Animesh Biswas

Abstract—**A new type of fin line discontinuity, which consists of a rectangular conducting strip placed transversely on the back side of the air dielectric interface containing the slot, is characterized in this work. Modeling of the fin line cavity containing the discontinuity is carried out using hybrid mode analysis, and then the Transverse Resonance Technique is used to extract equivalent circuit parameters of the discontinuity. Suitable sets of basis functions are chosen for accurately representing the field in the slot and the current on the strip. Calculated results are compared with the measured results for a sample discontinuity to validate the choice of the basis functions.**

I. INTRODUCTION

The off-slot discontinuity (discontinuity being in a plane which does not contain a slot) presented in this paper is useful in the realization of filter circuits. This type of discontinuity can also be used for providing dc bias to the active devices mounted across the slot. This paper presents an analysis of the off-slot discontinuity using the Transverse Resonance Technique proposed by Sorrentino and Itoh [1]. This technique involves application of the transverse resonance condition to a model of a fin line cavity containing the discontinuity. The accuracy of the equivalent circuit parameters of the discontinuity depends directly on the accuracy with which the resonant length of the cavity can be determined. This, in turn, depends on the accuracy of the assumed slot field distributions and strip current distributions. In this paper, besides using a rigorous hybrid mode analysis, suitable basis functions are chosen [2], [3] which account for the fringing fields at the edges. The validity of the assumed basis function is verified by measuring the transmission coefficient of sample discontinuity in the unilateral fin line and comparing it to the theoretical results. The discontinuity is used in realizing a filter by cascading it in the fin line, and the response is found suitable for a low-pass filter application [4].

Manuscript received August 19, 1993; revised November 10, 1994.

The authors are with the Department of Electrical Engineering, Indian Institute of Technology, Kanpur-208016, India.

IEEE Log Number 9410690.

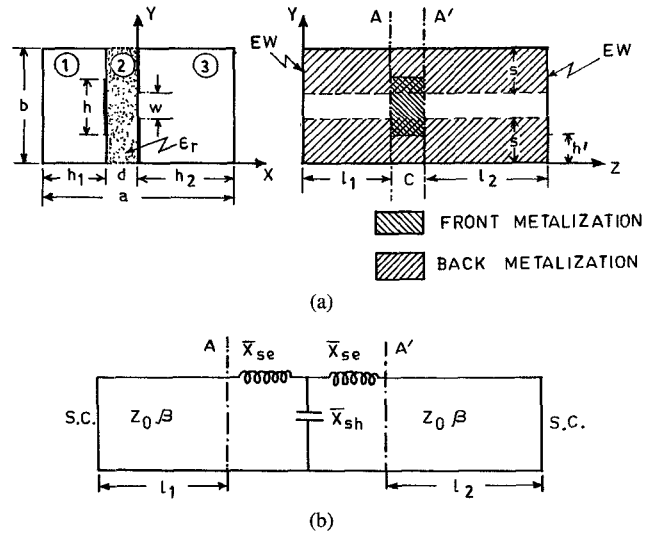

Fig. 1. (a) Cross-sectional and longitudinal views of a unilateral fin line cavity housing the off-slot discontinuity. (b) Equivalent circuit of (a).

II. ANALYSIS

Fig. 1(a) shows the cross-sectional and longitudinal views of a fin line cavity containing the off-slot discontinuity. The equivalent circuit of the fin line cavity with the discontinuity represented as a T-equivalent network is shown in Fig. 1(b).

A. Characteristic Equation of the Cavity

First, the fields in the three regions of the cavity [marked 1, 2, and 3 in Fig. 1(a)] are expanded in terms of modal fields with unknown coefficients. Then, by satisfying the boundary conditions followed by the application of orthogonality conditions at various dielectric–air interfaces, we can express all the field coefficients in terms of a transformed electric field at the slot aperture and currents on the conducting strip.

Next, by applying Galerkin's procedure, we get a set of homogeneous equations as

$$\sum_{p=0}^{P} C_{Ep} \sum_{m=1}^{\infty}\sum_{n=0}^{\infty} G_{11} L_{1emn}^{(p)} L_{2emn}^{(i)} + \sum_{q=0}^{Q} D_{Eq} \sum_{m=1}^{\infty}\sum_{n=0}^{\infty} G_{12} L_{2emn}^{(q)} L_{2emn}^{(i)} + \sum_{r=0}^{R} C_{Ir} \sum_{m=1}^{\infty}\sum_{n=0}^{\infty} G_{13} L_{1Imn}^{(r)} L_{2emn}^{(i)} + \sum_{s=0}^{S} D_{Is} \sum_{m=1}^{\infty}\sum_{n=0}^{\infty} G_{14} L_{2Imn}^{(s)} L_{2emn}^{(i)} = 0 \qquad i = 1, 2, \cdots, Q \tag{1a}$$

$$\sum_{p=0}^{P} C_{Ep} \sum_{m=0}^{\infty}\sum_{n=1}^{\infty} G_{21} L_{1emn}^{(p)} L_{1emn}^{(j)} + \sum_{q=0}^{Q} D_{Eq} \sum_{m=0}^{\infty}\sum_{n=1}^{\infty} G_{22} L_{2emn}^{(q)} L_{1emn}^{(j)}$$

$$+\sum_{r=0}^{R} C_{Ir} \sum_{m=0}^{\infty}\sum_{n=1}^{\infty} G_{23} L_{1Imn}^{(r)} L_{1emn}^{(j)}$$
$$+\sum_{s=0}^{S} D_{Is} \sum_{m=0}^{\infty}\sum_{n=1}^{\infty} G_{24} L_{2Imn}^{(s)} L_{1emn}^{(j)}$$
$$= 0 \qquad j = 1, 2, \cdots, P \tag{1b}$$

$$\sum_{p=0}^{P} C_{EP} \sum_{m=1}^{\infty}\sum_{n=0}^{\infty} G_{31} L_{1emn}^{(p)} L_{2Imn}^{(k)}$$
$$+\sum_{q=0}^{Q} D_{Eq} \sum_{m=1}^{\infty}\sum_{n=0}^{\infty} G_{32} L_{2emn}^{(q)} L_{2Imn}^{(k)}$$
$$+\sum_{r=0}^{R} C_{Ir} \sum_{m=1}^{\infty}\sum_{n=0}^{\infty} G_{33} L_{1Imn}^{(r)} L_{2Imn}^{(k)}$$
$$+\sum_{s=0}^{S} D_{Is} \sum_{m=1}^{\infty}\sum_{n=0}^{\infty} G_{34} L_{2Imn}^{(s)} L_{2Imn}^{(k)}$$
$$= 0 \qquad k = 1, 2, \cdots, S \tag{1c}$$

$$\sum_{p=0}^{P} C_{Ep} \sum_{m=0}^{\infty}\sum_{n=1}^{\infty} G_{41} L_{1emn}^{(p)} L_{1Imn}^{(l)}$$
$$+\sum_{q=0}^{Q} D_{Eq} \sum_{m=0}^{\infty}\sum_{n=1}^{\infty} G_{42} L_{2emn}^{(q)} L_{1Imn}^{(l)}$$
$$+\sum_{r=0}^{R} C_{Ir} \sum_{m=0}^{\infty}\sum_{n=1}^{\infty} G_{43} L_{1Imn}^{(r)} L_{1Imn}^{(l)}$$
$$+\sum_{s=0}^{S} D_{Is} \sum_{m=0}^{\infty}\sum_{n=1}^{\infty} G_{44} L_{2Imn}^{(s)} L_{1Imn}^{(l)}$$
$$= 0 \qquad l = 1, 2, \cdots, R \tag{1d}$$

where L_{1emn} and L_{2emn} are transformed slot field distributions and L_{1Imn} and L_{2Imn} are transformed strip current distributions. They are defined as follows:

$$L_{1emn} = \int_{y=0}^{b}\int_{z=0}^{l} E_z(y, z)|_{x=0} \sin(\alpha_n y) \cos(\beta_m z)\, dy\, dz \tag{2a}$$

$$L_{2emn} = \int_{y=0}^{b}\int_{z=0}^{l} E_y(y, z)|_{x=0} \cos(\alpha_n y) \sin(\beta_m z)\, dy\, dz \tag{2b}$$

$$L_{1Imn} = \int_{y=0}^{b}\int_{z=0}^{l} I_z(y, z)|_{x=-d} \sin(\alpha_n y) \cos(\beta_m z)\, dy\, dz \tag{2c}$$

$$L_{2Imn} = \int_{y=0}^{b}\int_{z=0}^{l} I_y(y, z)|_{x=-d} \cos(\alpha_n y) \sin(\beta_m z)\, dy\, dz. \tag{2d}$$

Also, "G" functions ($G_{11}, G_{12}, \cdots, G_{44}$) in (1) are derived in a similar way as given in [5].

Given a known fixed value of l_1, length l_2 can be computed from (1) by setting the determinant of the coefficient matrix equal to zero for a specified frequency and strip width.

After obtaining three sets of l_1 and l_2 for asymmetric discontinuity or two sets of l_1 and l_2 for symmetric discontinuity, the Transverse Resonance Technique [1] [as applied to Fig. 1(b)] is used to extract the equivalent circuit parameters of the discontinuity. $\overline{X}_{se}$ and $\overline{X}_{sh}$ in Fig. 1(b) are the normalized (with respect to dominant mode characteristic impedance of the fin line) equivalent series and shunt reactance of a symmetric discontinuity shown in Fig. 1(a), respectively, and Z_0 and β are the dominant mode characteristic impedance and the dominant mode propagation constant of the fin line.

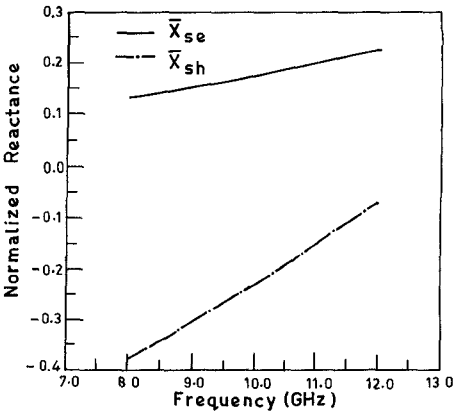

Fig. 2. Variation of equivalent circuit parameters with frequency: $a = 22.86$ mm, $b = 10.16$ mm, $d = 0.7937$ mm, $\epsilon_r = 2.22$, $h_1 = 10.6363$ mm, $W = 2.032$ mm, $h = 8.16$ mm, $h' = 1.0$ mm, $C = 2.0$ mm.

III. Choice of Basis Functions

The following basis functions for currents on the strip and the electric fields across the slot, which incorporate end effects, are chosen for the present problem

$$E_y(0, y, z) = (y - b/2)^{m-1}[(W/2)^2 - (y - b/2)^2]^{-1/2} \cdot \sin(n\pi z/l)$$
$$m = 1, 2, \cdots, M, \qquad n = 1, 2, \cdots, N \tag{3a}$$

$$E_z(0, y, z) = (y - b/2)^{p}[(W/2)^2 - (y - b/2)^2]^{1/2} \cdot \cos(q\pi z/l)$$
$$p = 1, 2, \cdots, P, \qquad q = 1, 2, \cdots, Q \tag{3b}$$

$$I_y(-d, y, z) = \frac{\sin[(2m-1)\pi/2(2y'/h+1)]}{[1-(2y'/h)^2]^{1/2}} (z')^{n-1} \cdot [(c/2)^2 - z'^2]^{-1/2}$$
$$m = 1, 2, \cdots, M', \qquad n = 1, 2, \cdots, N' \tag{3c}$$

$$I_z(-d, y, z) = \frac{\cos[(2p-1)\pi/2(2y'/h+1)]}{[1-(2y'/h)^2]^{1/2}} (z')^{q-1} \cdot [(c/2)^2 - z'^2]^{1/2}$$
$$p = 1, 2, \cdots, P', \qquad q = 1, 2, \cdots, Q' \tag{3d}$$

where $y' = y - b/2$ and $z' = z - (l_1 + c/2)$.

IV. Numerical Results

For wider strip widths ($c > 0.5$ mm), $m = n = 100$ in (1) gives an accuracy up to the third decimal place. For smaller strip widths, the same accuracy can be achieved by taking larger values of m and n (around 150), but then we will have to look for a compromise between accuracy and the computation time. The values of M, N, P, q, M', N', P', and Q' in (3) are also dependent on the accuracy required. We can fix their values as soon as the results start converging. We have determined their values for a sample width $c = 2.0$ mm as follows: $M = 1$, $N = 12$, $P = 1$, $Q = 12$, $M' = 2$, $N' = 2$, $P' = 2$, and $N' = 2$, and have reported the results.

Fig. 2 shows the variations of $\overline{X}_{se}$ and $\overline{X}_{sh}$ as a function of frequency in the X band. It is seen that series reactance increases and shunt reactance decreases with frequency. This could be because, with the increase in the frequency, the guide wavelength λ_g decreases, and hence the ratio c/λ_g increases, resulting in an increase in the series inductive reactance and a decrease in the shunt capacitive reactance.

The validity of the present theoretical results is confirmed experimentally by measuring the transmission coefficient for a sample discontinuity of width $c = 2.0$ mm in the X band. Fig. 3(a) shows

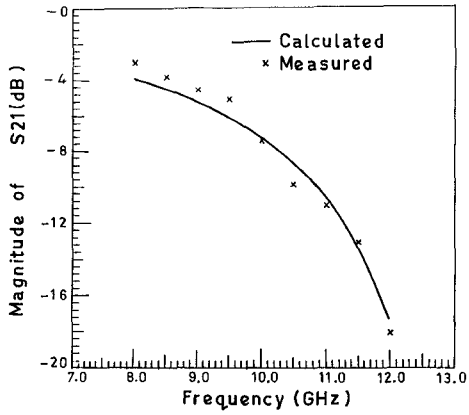

(a)

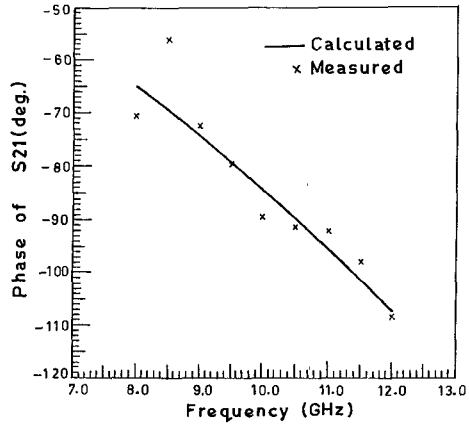

(b)

Fig. 3. Comparison of theoretical and experimental results of (a) magnitude of the transmission coefficient (dB) and (b) phase of the transmission coefficient (degree) $a = 22.86$ mm, $b = 10.16$ mm, $d = 0.7937$ mm, $\epsilon = 2.22$, $h_1 = 10.6363$ mm, $W = 2.032$ mm, $h = 8.16$ mm, $h' = 1.0$ mm, $C = 2.0$ mm.

a comparison of the theoretical and experimental results of $|S_{21}|$ in decibels, and Fig. 3(b) shows the comparison $\angle S_{21}$ in degrees of the sample discontinuity.

V. Conclusion

A new type of discontinuity in the unilateral fin line is analyzed using hybrid mode analysis in conjunction with the Transverse Resonance Technique. Appropriate basis functions are chosen to model the field in the slot and current on the discontinuity strip. Comparison curves of the transmission coefficient for a sample discontinuity are also presented. The two results are shown matching reasonably well, which validates the choice of basis functions.

References

[1] R. Sorrentino and T. Itoh, "Transverse resonance analysis of fin line discontinuity," *IEEE Trans. Microwave Theory Tech.*, vol. MTT-32, pp. 1633–1638, Dec. 1984.

[2] B. Bhat and S. K. Kaul, *Analysis Design and Application of Fin Lines.* Deadham, MA: Artech House, 1987.

[3] T. Itoh, "Spectral domain immittance approach for dispersion characteristics of generalized printed transmission lines," *IEEE Trans. Microwave Theory Tech.*, vol. MTT-28, pp. 733–736, July 1980.

[4] A. K. Gupta, "Characterization of two new types of fin line discontinuities," M.Tech. thesis, A.C.E.S., I.I.T., Kanpur, 1993.

[5] A. Biswas and B. Bhat, "Accurate characterization of an inductive strip in fin line," *IEEE Trans. Microwave Theory Tech.*, vol. 36, pp. 1233–1238, Aug. 1988.

Analysis of Spherical Radar Cross-Section Enhancers

John R. Sanford

***Abstract*—A method for determining the plane wave scattering by a spherical radar cross section enhancer is described. In the two-step process, the desired field representation is expressed as a superposition of vector spherical wave functions. This allows the plane wave scattering from a spherically stratified object to be determined.** *Love's equivalence principle* **is then employed to account for the metallic portions of the spherical reflector. The analysis utilizes the expansions of a plane wave, an electric current element, and a magnetic current element in terms of spherical wave functions. Measured results show fairly good agreement with predicted results.**

I. Introduction

Microwave passive reflectors are widely used to increase the radar cross section (RCS) of target drones or other test vehicles. An extremely effective RCS enhancer is a spherical dielectric lens with an angular sector covered by a conducting surface "cap." Such RCS augmenting devices are produced by a number of firms in Europe and the United States. The principle of the structure is as follows: The spherical lens has a permittivity that varies with radius. We choose a variation that causes the lens to focus a plane wave to a small area on the surface of the lens [1]. The cap reflects this energy back through the lens where it emerges as a plane wave, as depicted in Fig. 1. This combination of lens and cap serves as a passive reflector of microwave energy throughout a solid angle roughly equal to that subtended by the cap.

Here, we outline a method for determining the plane wave scattering by such reflectors. It is a two-step process. First, the desired field representation is expressed as a superposition of mode functions that are chosen in order to permit simple evaluation of the associated boundary conditions. This allows the plane wave scattering from the "capless" lens to be determined on the surface of the device. Afterwards, field equivalence is employed to determine the scattered field of the passive reflector. The analysis requires the expansion of a plane wave, an electric current element, and a magnetic current element in terms of spherical wave functions. The currents on the conductor are assumed to be those dictated by *the equivalence principle.*

II. Spherical Wave Function Expansions

In spherical coordinates, arbitrary fields are represented by a sum of vector spherical wave functions $\boldsymbol{m}$ and $\boldsymbol{n}$ as given by Stratton [2]

$$\boldsymbol{m}_{\substack{e \\ o}mn} = \mp \frac{m}{\sin\theta} Z_n(kr) P_n^m(\cos\theta) \begin{matrix}\sin \\ \cos\end{matrix} (m\phi)\hat{\theta}$$

Manuscript received February 18, 1994; revised September 29, 1994.

The author is with the Department of Microwave Technology, Chalmers University of Technology, 41296 Gothenburg, Sweden.

IEEE Log Number 9410698.